The Journal of Bone and Joint Surgery

Scientific Articles | May 5, 2014

Development of an Upper Extremity Fracture Model

Colin Dunn[1]; Lucas Haug[1]; Taylor Moehling[1]; Max Schultz[1]
Department of Biomedical Engineering, University of Wisconsin
1550 Engineering Dr. Madison, WI 53706

Abstract

An upper extremity fracture model would enable residents to learn how to reduce fractures, as well as experience applying and removing casts. After researching available sensors and applied force systems, the group found devices that could be functionally modified to serve as a solution to the problem. Through brainstorming and design matrices, the team decided on a final product incorporating a wooden dowel with a hinge system, force sensitive resistors (FSRs), an arduino microcontroller, Processing as the development environment to create a live visual display and Platsil as a tissue representation. The final design is an effective training tool that will determine the applied pressure and allow for a modular fracture resistance. A range of accepted pressure values for each sensor was calculated based on averages from the client Dr. Halanski. The acceptable range is displayed on the bar graph on the screen so the user knows whether they are applying acceptable pressures. In the future, data will be collected from multiple orthopedic surgeons to determine the variation of pressure applied during reduction.

Introduction

Dr. Matt Halanski of orthopedics and rehabilitation at the UW School of Medicine and Public Health submitted this project to the University of Wisconsin-Madison Biomedical Engineering Department. He served as the experienced orthopedic surgeon for the testing.

Fractures are common in pediatrics, representing a major public health problem. Between 0 and 16 years of age, 42% of boys and 27% of girls experience at least one fracture and 84% of those fractures are upper limb fractures [1].

Currently there are not any commercially available models to teach residents how to properly apply and remove a cast from a fracture. The most serious complication of casting is compartment syndrome which is a condition of increased pressure within a closed space that impairs blood flow and tissue perfusion which leads to slow or incomplete bone healing. Thermal injuries to the skin can also occur due to high temperatures reached during molding of the cast. The most common related problem is skin breakdown which may be caused by pressure from a wrinkled, unpadded or under-padded area of the arm [2].

Forearm injuries are very common, counting for 40% of all pediatric fractures. The peak occurrence is when the child is greater than 5 years of age when the bone is weakest due to velocity of growth. The radius is a curved bone in the proximal third that is flat distally. The ulna has a triangular shape throughout, with an apex in the proximal third. The two bones are stabilized distally and proximally by the triangular fibrocartilage complex and the annular ligament [3]. Most forearm fractures occur in the radius but sometimes can be both a radial and ulnar fracture. Distal radius fractures account for 75% of all forearm fractures in children. Often distal radius fractures, seen in Figure 1, are accompanied by a wrist fracture due to contact, such as a fall on an extended arm [4]. Forearm fractures can be caused by indirect or direct contact. Indirect contact involves a fall in which a flexion injury causes dorsal angulation and an extension injury causes volar angulation. Direct contact involves trauma to the radial or ulnar shaft [3]. In distal fractures, the proximal part will be in neutral or slight supination. The weight of the hand and the pronator quadratus pronates the distal fragment [5].

Figure 1: Distal radius fracture in pediatric patient

The goal for the team was to create a radius-only distal fracture that allows varying resistance. It would be beneficial to mimic a greenstick fracture since it is the most common fracture found in children. From research, the team decided these criteria would benefit the largest population of pediatrics. It is important to allow traction, angulation and rotation in order to create an acceptable learning tool for residents to assist them in various types of fractures that they will experience.

Materials and Methods

Experimental Model

The first iteration of the final design consisted of a modular resistance system, a soft tissue representation, and circuitry, and a software component. A hinge system, as seen in Figure 2, composed of a wooden dowel, was used to represent the modular resistance system. The wooden dowel was used as a proof of concept, as well as to provide the team with a working representation of a fracture for testing the sensors. The soft tissue representation was created by a previous BME design team and was made using Platsil Gel-10, which has viscoelastic mechanical properties similar to skin and muscle. The tissue representation was molded from the arm of a female pediatric patient. The measurements of the pressure along the forearm fracture model were accomplished by FSRs. Ten 1.27 cm (0.5 inch) diameter FSRs were placed on the model based on recommended locations from the client. The output voltage for each resistor was sampled using an arduino Mega2560.

Figure 2: Platsil arm model and wooden dowel fracture system

This device was programmed to read the voltage at each analog input, and an array was formed. A Java extension called Processing was used to display the data from the FSRs in a color-coded graphical representation shown in Figure 3.

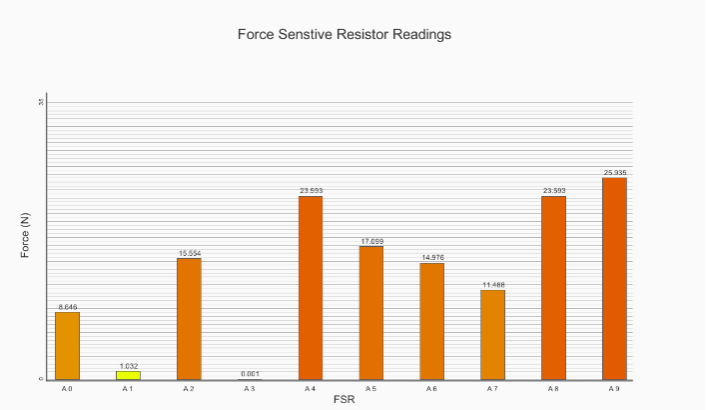

Figure 3: Processing displaying live bar graphs with force output for each sensor

Model Validation

Two tests were conducted to verify the accuracy of the sensors and prove the variable resistance capabilities of the fracture. The first test used a 100 gram weight to apply point loads to various locations on the FSRs; this helped to show that by placing 1.27 cm (0.5 inch) rubber cabinet stoppers on the FSRs that the force can be focused and distributed across the entire FSR as seen in Figure 4. The second test performed was varying the resistance of the modular system. By varying the tightness of the system at the hinge, the torque needed to reduce the fracture varied; however, this method did not prove to be fully reliable and consistent as seen in the data table in the Appendix. Due to the change in direction of the project, the second iteration of the final design will not be using all of the components of the first iteration. The second iteration will have a fracture model professionally developed by a separate company while the focus of the project is now to develop a mobile pressure mapping system that will form fit to any model.

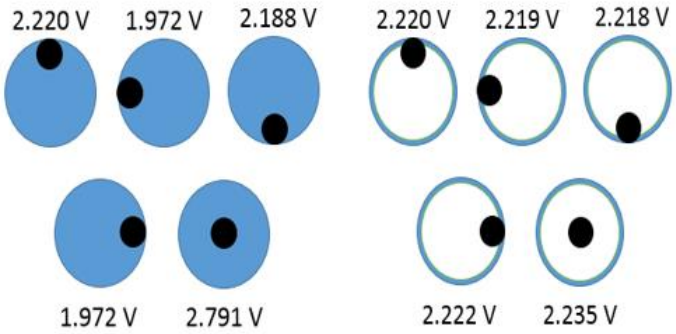

Figure 4: Test with (right) and without (left) bumpers to determine force output when loads were applied at various locations on the sensor

Model Modifications

Since the client moved to other sources for bone and tissue representation in this model, the scope and focus of the project was altered. The main goal was to create pressure mapping hardware and software for use on multiple limb fracture models of varying sizes and shapes. This new scope required a complete retooling and rethinking of the design of the pressure gathering and graphing system. The new model can be broken into two distinct sections: the hardware system and corresponding software to create an intuitive visual display of the data gathered.


Figure 5: Metal tray with most sensor coverage on distal and proximal ends due to hand placement during reduction

The new hardware system utilizes an Under Armour spandex fabric with

three metal trays, seen in Figure 5, containing five FSRs each that are slid in between layers of fabric. The trays are 1.27 cm (0.5 inch) wide and 20.32 cm (8 inch) long and made of thin galvanized steel. The three trays are equally spaced around the circumference of the sleeve. The fabric allows near universal use of the device on limbs of different sizes because of the ability to reversibly deform. The FSRs have a sensing area of 9.53 mm (0.375 inches) with a force range of 0-100lbs. They are covered with 9.53 mm (0.375 inch) half-spherical acrylic balls that have a reduced vertical profile compared to the last design. These acrylic pieces will gather the normal component of all forces applied within one radian to increase efficacy and accuracy of the data gathering technique. There are five FSRs on each tray, with clustering near the distal and proximal ends based on standard hand positioning for fracture reduction as stated by the client.

The live software component was created using Processing to qualitatively demonstrate pressure to the user. Through testing the client, an orthopedic surgeon, the baseline pressure ranges were created (shown in Figure 6 as clear boxes outlined in black). When the user applies pressure, one of three colors appear. When the user is applying too little pressure to a specific sensor, the bar will be blue. When the applied pressure is too high, the bar will be red. However, when the pressure is within the baseline range, the color of the bar will be green. This allows the user to obtain real-time feedback for pressure applied on each sensor which leads to self-correction of the technique or hand placement.

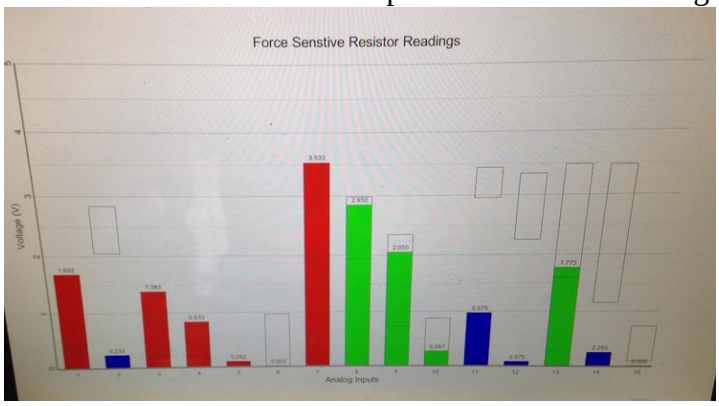

Figure 6: Computer display in Processing using new color scheme

Testing

Dr. Matt Halanski, an orthopedic surgeon at the University of Wisconsin-Madison Hospital, reduced the fracture on the prototype a total of 20 times. The subject was blind from viewing his individual results, which eliminated any chance for bias. The completion of the test was marked when Dr. Halanski believed the pressure applied was enough to reset the fracture based on experience and feel.

Data Analysis

The data was sampled at each sensor every 10 ms into a text file. The file was imported into MatLab for further analysis. For each of the 20 trials, the maximum pressure value was recorded and averaged for each of the 15 sensors. This is demonstrated in Graph 1. Also, the standard deviation was calculated of the maximum pressures for each sensor, and can be seen in Graph 1 as the upper and lower error bars. If the value of the lower error bar was below zero, the value was rounded to zero since a negative value would be irrelevant. The calculated data is shown in Table 1 below:

Sensor	1	2	3	4	5	6	7	8	9	10	11	12	13	14	15
Mean Value (Volts)	0.044	2.442	0.549	0.027	1E-03	0.163	0.185	2.46	1.535	0.386	3.199	2.796	2.535	2.312	0.41
SD (Volts)	0.157	0.393	0.335	0.051	0.004	0.479	0.722	0.52	0.813	0.434	0.241	0.538	0.94	1.161	0.32
Upper Range	0.201	2.835	0.884	0.079	0.005	0.642	0.907	2.98	2.348	0.82	3.44	3.334	3.475	3.473	0.73
Lower Range	0	2.049	0.214	0	0	0	0	1.94	0.723	0	2.958	2.258	1.595	1.151	0.09

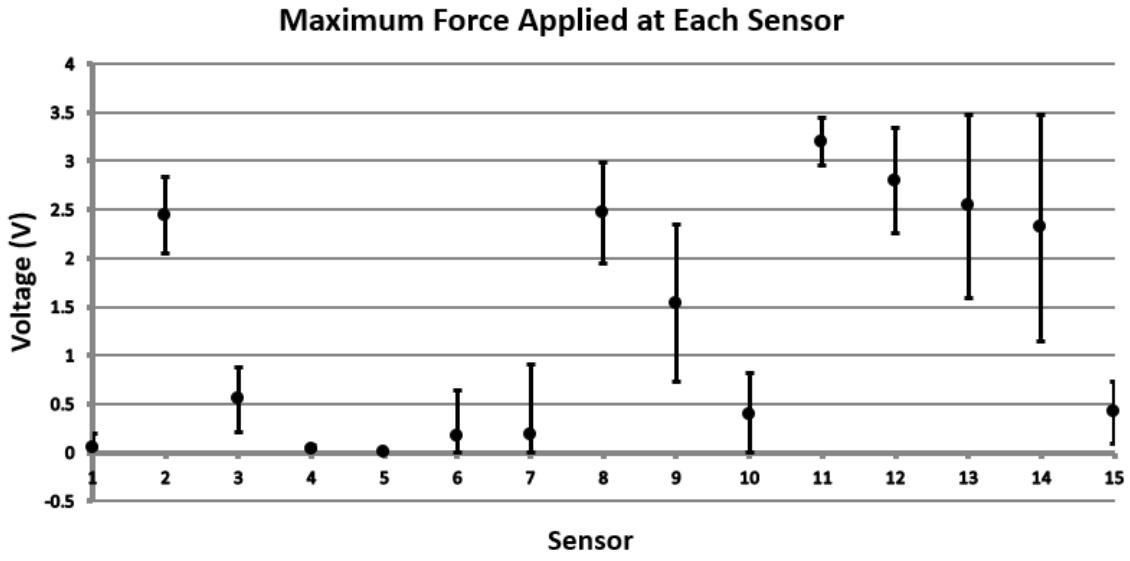

Graph 1: Average maximum pressure applied at each sensor over 20 trials

Results

Based on the data, Dr. Halanski demonstrated consistency when reducing a fracture due to the fact that he applied pressure on the same sensors each time. Also, the standard deviations for each of the sensors implied consistency among the trials with only a few outliers. This indeed proves the notion that Dr. Halanski has mastered a specific technique that is both effective and uniform. This data will be useful for teaching proper technique to residents.

Source of Funding

The funding for this project came from the client, Dr. Matt Halanski and the Department of Orthopedics and Rehabilitation at the University of Wisconsin-Madison Hospital. There was no limit for funding as long as the purchases were approved by the client, however, it was the team goal to minimize costs to under $500.

Discussion

The average maximum pressures for each sensor over 20 trials and standard deviation of the maximum pressures at each sensor were used to create baseline ranges for each sensor on the computer display (Figure 6). These ranges were intended to be used as a qualitative reference for users of the fracture model. A major problem is that residents will unlikely use the same hand positioning that was used during testing. In the future, reference points for hand placement should be implemented on the sleeve to ensure users place hands in optimal positions for sensor contact and proper reduction.

In the future, more testing should be performed in order to optimize the location of the sensors. This, along with ideal hand placement positions will allow for an optimal number of sensors to be used during fracture reduction, and therefore more effectively provide useful feedback to the users. One concern, however, is that hand sizes vary among doctors; therefore, this will be essential to keep in mind while determining the proper hand locations on the sleeve, as well as, the optimized sensor locations.

Once the hand and sensor locations are optimized, a significant amount of testing should be completed by multiple orthopedic surgeons to determine variance among skilled professionals. If pressure ranges are similar, it will be possible to obtain more accurate pressure ranges for reducing a fracture. If pressure ranges are very different, this proves that each orthopedic surgeon has a unique technique which would lead back to the drawing board. After preliminary testing, the model should be tested by a spectrum of residents to determine improvements for usability and functionality.

Lastly, a visual representation of the forearm model with the sensor locations should be incorporated into the program and the pressure sensing system should be made wireless. Having a visual representation of the forearm with the sensor locations incorporated with the pressure data would allow for immediate feedback and improve the learning process for residents while using the model.

Acknowledgements

The design team would like to give special thanks to Professor Mitch Tyler and the UW Madison Biomedical Engineering Department for guidance and input throughout the entire design process. Additionally, special thanks to the client Dr. Matt Halanski for providing the team with the existing prototype and insight on future work. The team would like to thank Professor John Kao for helping with biomaterials research. It is important to recognize Gabe Bautista and Professor Tom Yen of the design team last year for meeting with the team to discuss past progress. The team would like to thank Shlomi Laufer and Dr. Carla Pugh's lab for information regarding sensors and microcontrollers. Also, it is important to acknowledge the College of Engineering Student Shop for providing assistance with the fabrication of the hinge system. Lastly, special thanks go out to Michael Bauer for assistance with programming and understanding of Processing and the arduino code.

References

[1] Biomed Central. (October, 2010 30). *Pattern of fractures across pediatric age groups: analysis of individual and lifestyle factors*. Retrieved from http://www.biomedcentral.com/1471-2458/10/656

[2] Boyd, A. (2009, January 01). *Principles of casting and splinting*. Retrieved from http://www.aafp.org/afp/2009/0101/p16.html

[3] Egol, K. (2010). *Handbook of fractures*. (4th ed.). Lippincott Williams & Wilkins. Retrieved from https://www.inkling.com/store/book/handbook-of-fractures-egol-4th/?chapterId=67acab6e9bda41e7ba5d8538cf48d75c

[4] Wright, M. (July, 2010 16). *Forearm injuries and fractures*. Retrieved from http://www.patient.co.uk/doctor/Forearm-Injuries-and-Fractures.htm

[5] Bernstein, R. (2010). *Pediatric forearm and distal radius fractures*. Retrieved from http://www.togct.com/downloads/bernstein/Pediatric-Forearm-Fractures.pdf

Appendix

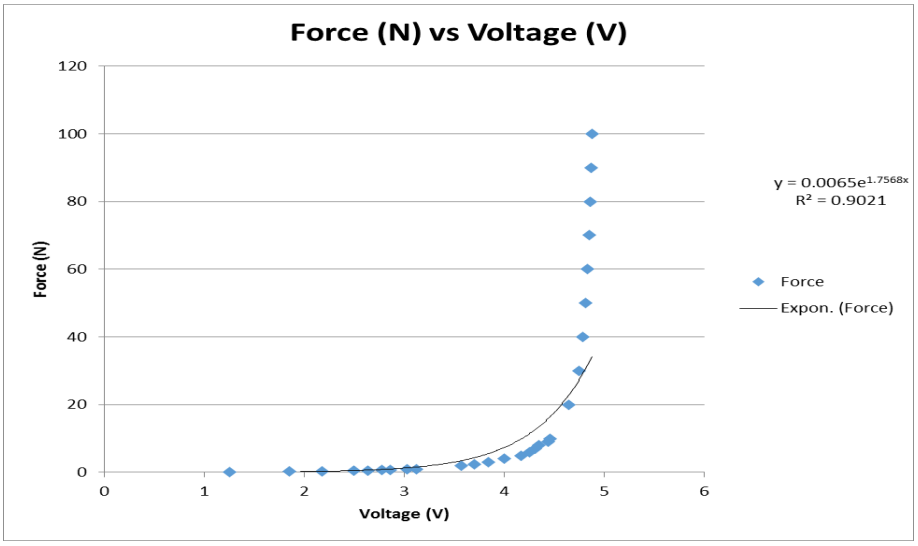

Figure 1: Calibration curve for 10 original FSR sensors using various weights

# of turns from tight	FSR 1	FSR 2	FSR 3	FSR 4	FSR 5	FSR 6	FSR 7	FSR 8	FSR 9	FSR 10	Average
0	8.646	1.032	15.554	0.001	23.593	17.009	14.976	11.488	23.593	25.935	14.183
0.25	6.759	3.891	13.512	0.0256	18.416	14.463	10.513	9.463	17.156	10.163	10.436
0.50	6.846	4.315	8.546	0.001	12.56	9.463	12.456	5.11	8.61	5.163	7.307
0.75	2.546	0.786	1.563	0.0003	13.156	0.001	5.419	6.13	0.163	0.135	2.9899
1.00	0.001	0.303	0.529	1.179	12.629	0.001	2.88	0.052	0.003	0.24	1.7817

Figure 2: Table displaying force data from each sensor required to reduce a fracture at various resistances using the hinge to tighten

Figure 3: Dr. Halanski's hand placement while reducing a fracture using previous model

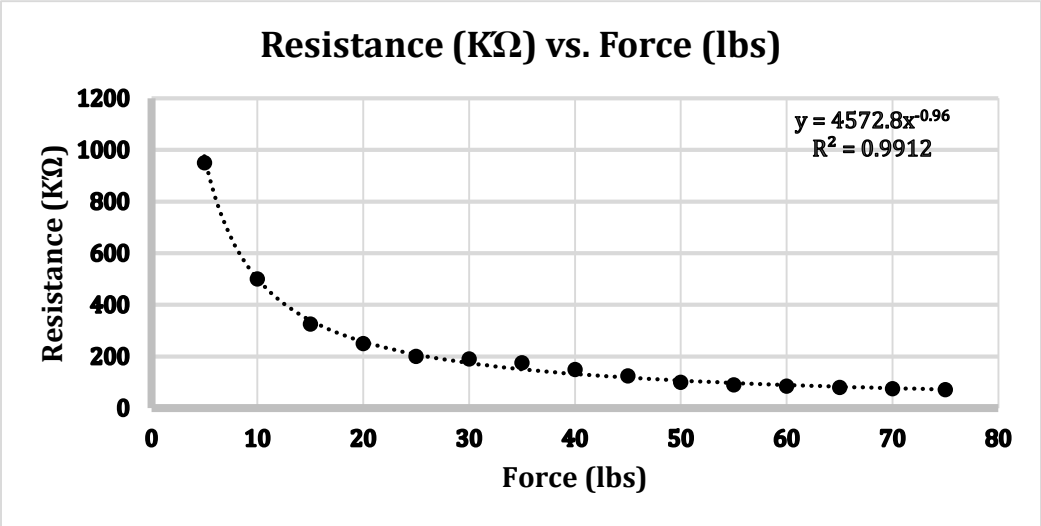

Figure 4: Calibration curve for new FSRs

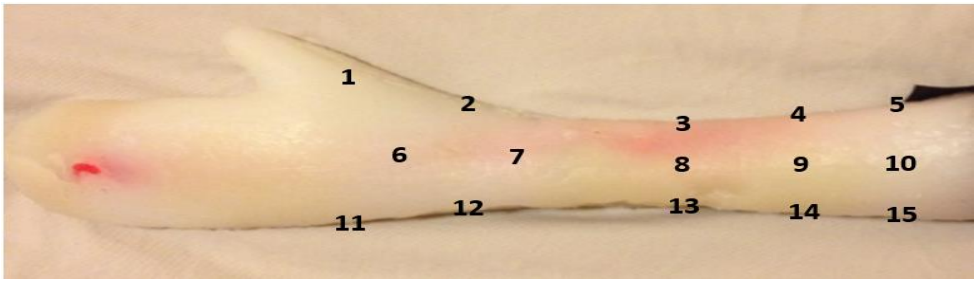

Figure 5: Location of FSRs on Platsil arm

Figure 6: Final model with sleeve